PCCP

Accepted Manuscript

ROYAL SOCIETY OF CHEMISTRY

www.rsc.org/pccp

Cooperativity in Beryllium Bonds

Ibon Alkorta,* Jose Elguero

Instituto de Química Médica (CSIC), Juan de la Cierva, 3, 28006-Madrid, Spain

Manuel Yáñez, Otilia Mó

Departamento de Química, Módulo 13, Universidad Autónoma de Madrid, Campus de Excelencia UAM-CSIC, Cantoblanco, 28049 Madrid, Spain

* Author to whom correspondence should be addressed.

e-mail: ibon@iqm.csic.es

Abstract

A theoretical study of the beryllium bonded clusters of the (iminomethyl)beryllium hydride and (iminomethyl)beryllium fluoride [HC(BeX)=NH, X = H, F] molecules has been carried out at the B3LYP/6-311++G(3df,2p) level of theory. Linear and cyclic clusters have been characterized up to the decamer. The geometric, energetic, electronic and NMR properties of the clusters clearly indicate positive cooperativity. The evolution of the molecular properties, as the size of the cluster increases, is similar to those reported in polymers held together through hydrogen bonds.

Table of contents entry

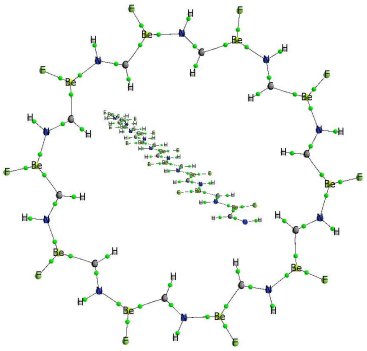

Positive cooperativity is found in Beryllium bonded complexes similar to that described for hydrogen bonded systems.

Introduction

Among the increasing number of weak interactions described in the recent years, the beryllium bond corresponds to strong interaction energies.[1] As conventional hydrogen bonds, beryllium bonds are stabilized by the concomitant contribution of both electrostatic and covalent-like effects.[1] The electropositive character of Be and its relatively high net positive charge favors significantly strong electrostatic interactions with the basic site of the Lewis base, which bears a negative net charge; but the most important contributor to the stability of these closed-shell interactions is the charge donation from the lone-pairs of the Lewis base towards the empty *p* orbitals of beryllium and the σ_{BeX}* antibonding orbitals. Accordingly, two of the signatures of beryllium bonds is the bending of the BeX_2 Lewis acid and the lengthening of its BeX bonds.[1] The aforementioned charge donation deeply affects also the intrinsic properties of the Lewis base, through a significant electron density redistribution, which usually have dramatic effects in its electron donor-acceptor capacity and accordingly on its intrinsic basicity and acidity.[1-11] For instance, typical bases as aniline or formamide can be changed in stronger acids than phosphoric or chloric acids, through the formation of beryllium bonds with $BeCl_2$. Similarly, water, methanol and SH_2 become stronger acids than sulfuric acid, pyridine becomes a C acid almost as strong as acetic acid, and unsaturated hydrocarbons such as ethylene and acetylene become as strong an acid as nitric or sulfuric acids, respectively.[8] The complexation with $BeCl_2$ of hydrogen bonded dimers can produce the spontaneous proton transfer.[10, 11]. In addition, the complexes where the beryllium bond is present can be considered as a model for some of the interactions responsible of the stabilization in the so called metal-organic-frameworks (MOFs).[12]

Cooperativity effects are one of the signatures of weak interactions, especially hydrogen bonds, HBs.[13-46] These effects are manifested by a strengthening of the HB between the HB donor and the HB acceptor, when one of them or both, interact with a third HB donor or HB acceptor. The possibility of having cooperative effects among HB and other different non-covalent interactions have been reviewed recently.[47]

The question that we want to address in this article is whether cooperativity can be found in chains of complexes attached via beryllium bonds and, in case it is found, if they show similar characteristics to those described for other weak interaction clusters. For that purpose, the linear and cyclic polymeric structures of **1H** and **1F** (Scheme 1)

including up to 10 monomers have been characterized by means of B3LYP density functional theory (DFT) method.

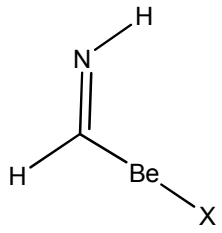

X = H **1H**
X = F **1F**

Scheme 1. Molecules considered in the present study.

Computational methods

The B3LYP density functional approach,[48, 49] which combines the three-parameter hybrid exchange functional of Becke with the non-local LYP correlation functional have been used for all the calculations. For the geometry optimizations a 6-31+G(d,p) basis set has been used,[50] whereas to obtain more reliable final energies a larger 6-311++G(3df,2p) basis set[51] expansion was employed. Harmonic vibrational frequencies, obtained at the B3LYP/6-31+G(d,p) level were used to classify the stationary points found as local minima of the potential energy surface. This theoretical model has been shown to adequately reproduce the characteristic of conventional inter- and intra-molecular HBs and Beryllium bond in comparison with the results obtained through high-level ab initio CCSD(T) calculations.[1, 52, 53] These calculations have been carried out with the Gaussian-09 program.[54]

There are different procedures to analyze the non-covalent interactions, most of them based on an analysis of the electron density. In this study we will use two complementary approaches, namely the atoms in molecules (AIM) theory,[55, 56] and the natural bond orbital (NBO) approach.[57] AIM, permits to define the molecular graph of the investigated systems as the ensemble of maxima of the electron density, ρ, associated with the position of the nuclei, saddle points, in which ρ, has two negative and one positive curvatures, the so called bond critical points (BCPs) and the zero gradient lines connecting them, or bond paths. The value of the electron density at the

BCP, ρ_b, for inter and intramolecular HBs[45, 58-68] and for beryllium bonds, as well, is a good quantitative measure of the strength of the bond. The AIMAll program[69] has been used for the AIM analysis.

The NBO method is based on the use of localized atomic hybrids, obtained as block eigenvectors of the one-particle density matrix, which are characterized by their occupation numbers. Once these molecular orbitals are obtained, it is possible to evaluate the second order interaction energies between occupied and empty orbitals, which would be a measure of the charge transfer from the former to the latter, and to calculate the Wiberg bond order,[70] which is another useful way of quantitatively define the strength of a linkage. The NBO-6[71] connected to the Gaussian09 program has been used for these calculations. The NBO orbitals have been plotted with the Jmol program[72] using the tools developed by Marcel Patek.[73]

The NMR absolute chemical shielding has been calculated with the GIAO method[74, 75] using the facilities of the Gaussian-09 program.

Results and Discussion

Structure and Bonding

A minimum structure has been found for all the linear chains while maintaining C_s symmetry. In the case of the cyclic structures, S_4 symmetry is found in the tetramer, C_1 in the pentamer and C_{nH} for the rest of the clusters (n = 6-10).

The optimized geometries of the linear and cyclic hexamer of **1H**, as representative examples, are show in Figure 1 while those of all the remaining clusters are included in the Supporting Information Material.

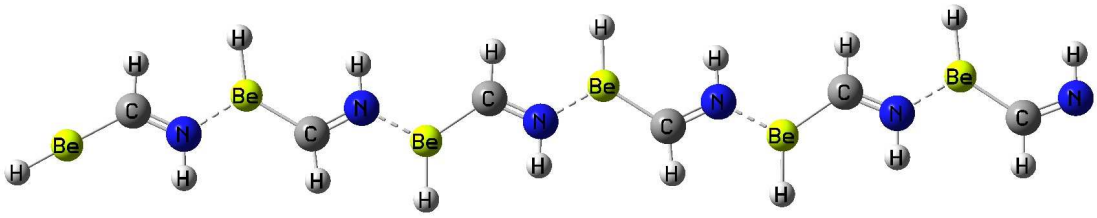

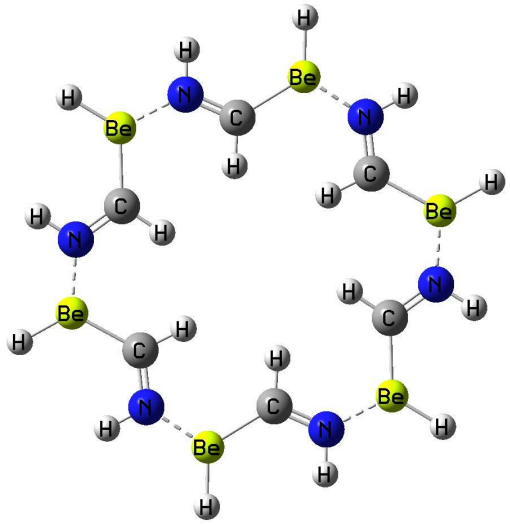

Figure 1. Optimized geometries of the linear and cyclic hexamer of **1H**.

The N···Be and C-Be interatomic distances for all the systems have been gathered in Tables S1 of the Supporting information material. The longest N···Be interatomic distances are found in the $(\mathbf{1H})_2$ and $(\mathbf{1F})_2$ dimers with values of 1.738 and 1.750 Å, respectively, while the shortest distance is obtained in the central N···Be interaction of the decamer, with values of 1.670 and 1.672 Å for the H and F series, respectively, already pointing to significant cooperative effects. For comparative purposes, the N···Be distances in all the linear complexes of **1H** have been represented in Figure 2, as a function of the position of the interacting monomers along each chain. The evolution of the N···Be interatomic distances obtained for the linear clusters of **1F** is similar to those of **1H** (see Figure S1 of the Supporting Information Material). Figure 2 clearly shows that the shortest intermolecular distances are those between the monomers in the center of the chain and the longest between the monomers at the two ends of the chain. This shortening effect is more important the longer is the chain. A similar behavior has been described for hydrogen and dihydrogen bonds chains[76-79] and it has been correlated with the cooperativity effect observed in those systems.

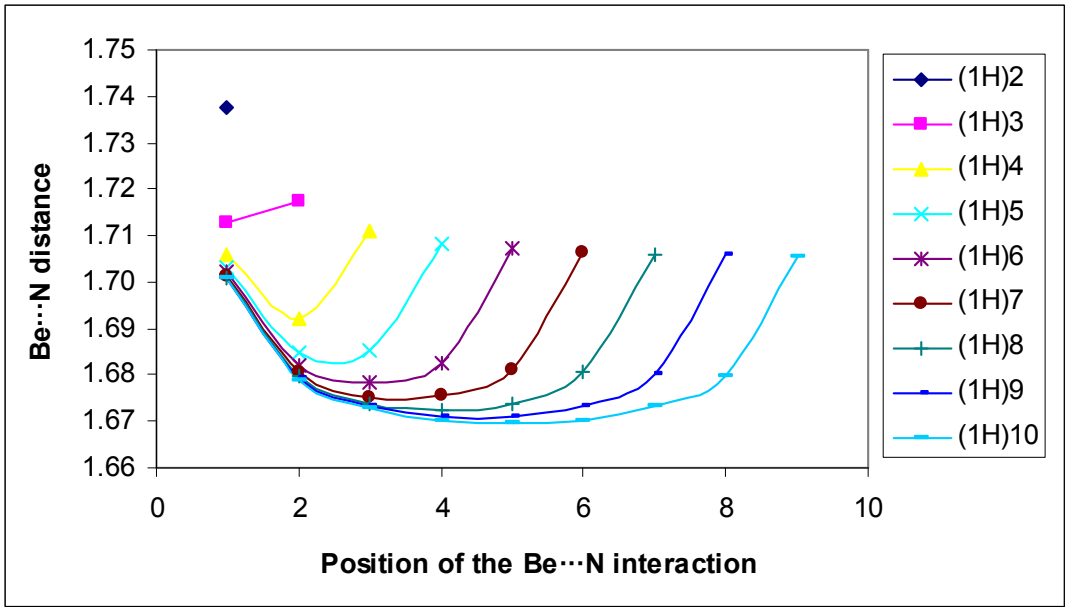

Figure 2. Evolution of the Be···N distance (Å) in the linear chain of the **1H** clusters.

These clear cooperative effects lead to the strengthening of the Be···N bond between the central monomers when the length of the chain increases. Indeed, the NBO analysis indicates that the bonding between the two monomers in the dimer arises from a significant charge transfer from the lone pair of the imino nitrogen atom towards the empty orbitals of the beryllium atom (Be-C σ*, Be-H σ* and Be p*), reflected in very large second order orbital interaction energies (See Figure 3). However, these interaction energies, which for the $(\mathbf{1H})_2$ dimer amount 53.9, 54.1 and 60.6 kJ mol^{-1}, respectively, increases dramatically when the length of the chain increases, being as large as 72.6, 58.3 and 83.6 kJ mol^{-1} between the central monomers of the decamer $(\mathbf{1H})_{10}$, due to two concomitant effects, the increase of the intrinsic basicity of the imino nitrogen and the enhancement of the intrinsic acidity of the BeX group. These charge transfers make that in the dimer the imino molecule acting as electron donor is positively charged (+ 0.046 e) whereas the one acting as electron acceptor is negatively charged. In the case of longer chains, the charge of the inner monomers is nearly zero because they act as electron donors and electron acceptors, simultaneously. However, the charge of the extreme molecules increased reaching values of ±0.068 e in $(\mathbf{1H})_{10}$.

Similar interactions are also found in the cyclic polymers with the difference that their values are obviously the same for each pair of monomers. Although the values of the

interaction energies are not significantly different from those obtained for the linear analogues, the stabilization effect is smaller due to a less effective overlap between the interacting systems, due to the cyclic arrangement of the overall structure.

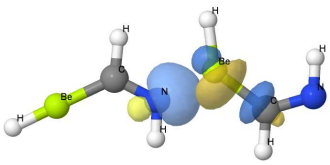

N(lp) → Be-C σ*
53.9 kJ/mol

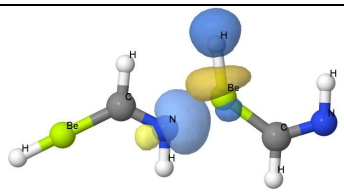

N(lp) → Be-H σ*
54.1 kJ/mol

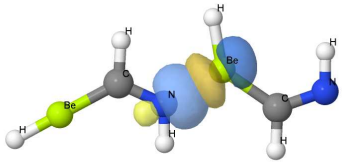

N(lp) → Be p*
60.6 kJ/mol

Figure 3. NBO orbitals involved in the beryllium bond of $(\mathbf{1H})_2$. The stabilization due to the charge transfer is indicated.

The significant charge transfer to the σ_{CBe}* antibonding orbital results in an elongation of the C-Be distances (See Figure 4 for the linear **1H** clusters), being this effect more pronounced in the center of the chain and in the larger clusters, as mentioned above.

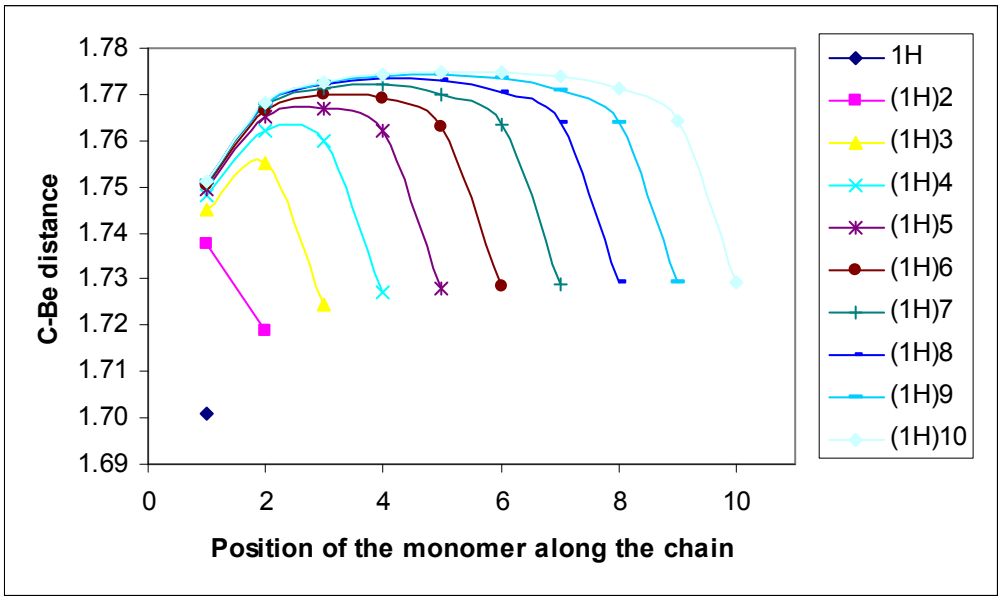

Figure 4. Evolution of the C-Be distance (Å) in the linear chain of the **1H** clusters. (Figure S2 represents the evolution of the C-Be distance for the linear **1F** clusters).

These structural changes are also reflected in the force field of the polymers investigated. For instance, for the $(\mathbf{1H})_2$ dimer the BN and the CBe stretching vibrational modes are estimated to appear at 687 and 880 cm^{-1}, respectively. On going to the decamer $(\mathbf{1H})_{10}$, these vibrational modes appear coupled, but whereas the BN stretching of the central monomers is significantly blue-shifted (from 187 to 201 cm^{-1}) that involving the extreme monomers is slightly red-shifted (8 cm^{-1}). Similarly the CBe stretching for the central monomers is significantly shifted to the red by ca. 90-115 cm^{-1}, whereas for that involving the extreme monomer this shifting is only 8 cm^{-1}.

It is then obvious that the greater the strength of the Be···N interaction the longer the C-Be bonds. Actually, it is possible to obtain linear correlations between the N···Be and the C-Be bond distances, but it is necessary to group the points in different families according to their relative position within the polymer, as shown in Figure S3 of the SI for the **1H** clusters. Consistently, the bond orders of the Be-N interaction parallel the interatomic distances previously discussed and range from 0.12 in $(\mathbf{1H})_2$ to 0.15 in the shortest Be-N bond of $(\mathbf{1H})_{10}$. In the same way, the Be-C bonds are weakened going from 0.37 in $(\mathbf{1H})_2$ to 0.28 in $(\mathbf{1H})_{10}$.

In the cyclic systems, both the Be-C and Be···N interatomic distances tend to be smaller as the size of the ring increases. This effect is larger in the Be···N distances than in the Be-C ones.

The charge transfer towards the empty p orbital of Be leads to a change in the hybridization of Be atom and accordingly to a bending of the C-Be-X group which is strictly linear in the isolated monomer and bents up to 120º in some of the complexes.

These cooperative effects will also be observed in the interaction energies, in the topology of the electron density and in the magnetic properties of the polymers as discussed in forthcoming sections.

Energies

The interaction energies for the linear and cyclic clusters have been calculated at the B3LYP/6-311++G(3df,2p)//B3LYP/6-31+G(d,p) computational level using Eq. 1 and they have been gathered in Table 1. The energetic results obtained with the smaller

basis set, B3LYP/6-31+G(d,p) (see Table S2 of the Supporting Material) are always slightly larger than those obtained with the larger basis set but both set of values show an almost perfect linear relationship (R^2=0.999). In the rest of the article only the energetic values obtained at the B3LYP/6-311++G(3df,2p)//B3LYP/6-31+G(d,p) computational level will be considered.

In all the cases studied here, the cyclic configuration is more stable than the corresponding linear one, both in terms of electronic energies and in terms of free energies. It should be noted that the gap between cyclic and linear polymers decrease when evaluated in terms of free energies because the cyclic structures are entropically disfavored. However, the extra beryllium bond present in the cyclic structures more than compensate the entropic stability loss. Second order polynomial relationships are found between the energetic differences in the linear and cyclic complexes (Fig. 5). The maximum difference is observed in the heptamer for X=H if energies are used and for the hexamer if free energies are employed. For the fluorinated derivative both energetic magnitudes predict the octamer to be most stable in relative terms.

$$E_i = E_{complex}(\mathbf{1X})_n - n*E(\mathbf{1X}) \qquad \text{Eq. 1}$$

Table 1. E_i Interaction energy (kJ mol^{-1}) of the linear and cyclic structures calculated at the B3LYP/6-311++G(3df,2p) computational level. ΔE_{lc} (kJ mol^{-1})[a] stands for the energy difference between the cyclic and the linear isomers.

	X = H			X = F		
System	Linear	Cyclic	ΔE_{lc}	Linear	Cyclic	ΔE_{lc}
$(\mathbf{1X})_2$	–119.0			–115.3		
$(\mathbf{1X})_3$	–274.0			–268.4		
			–190.3			–173.7
$(\mathbf{1X})_4$	–441.3	–631.6	(–161.3)	–434.0	–607.7	(–149.8)
			–235.6			–222.5
$(\mathbf{1X})_5$	–614.4	–850.0	(–208.0)	–605.6	–828.1	(–194.6)
			–257.8			–254.4
$(\mathbf{1X})_6$	–790.1	–1047.9	**(–226.8)**	–780.2	–1034.6	(–225.4)
			–267.1			–269.3
$(\mathbf{1X})_7$	–967.5	–1234.6	(–223.5)	–956.2	–1225.5	(–231.0)
			–263.2			**–271.7**
$(\mathbf{1X})_8$	–1145.6	–1408.8	(–214.2)	–1133.0	–1404.7	**(–238.6)**
			–252.1			–266.5
$(\mathbf{1X})_9$	–1324.5	–1576.6	(–210.0)	–1311.2	–1577.7	(–221.1)
			–235.5			–256.9
$(\mathbf{1X})_{10}$	–1503.5	–1739.0	(–222.6)	–1489.2	–1746.1	(–222.9)

[a] The values within parenthesis correspond to the differences in terms of free energies.

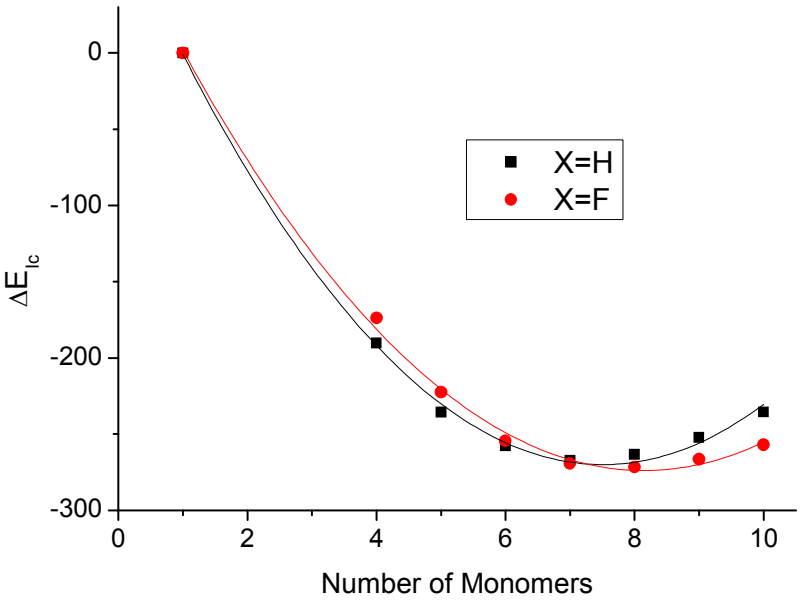

Fig. 5. Energetic difference between the linear and cyclic complexes (kJ/mol) vs. the number of monomers. The fitted second order polynomial relationships show R^2= 0.998 for both X=H and F.

The cooperativity effects on the interaction energy can be evaluated in several different ways. Here we have calculated the interaction energy per monomer (Eq. 2) and the incremental interaction energy ΔE_i as defined in Eq. (3) (See Table 2)

E_i per monomer = E_i/n Eq. 2

$\Delta E_i = E_{complex}(\mathbf{1X})_n - E_{compex}(\mathbf{1X})_{n-1} - E(\mathbf{1X})$ Eq. 3

Table 2. Interaction energy per monomer (Eq. 2) and increment of interaction energy (Eq. 3) (kJ mol^{-1}) in the $(\mathbf{1H})_n$ and $(\mathbf{1F})_n$ linear and cyclic clusters.

	X = H				X = F			
	Linear		Cyclic		Linear		Cyclic	
System	E_i/n	ΔE_i	E_i/n	ΔE_i	E_i/n	ΔE_i	E_i/n	ΔE_i
$(\mathbf{1X})_2$	–119.0	–119.0			–115.3	–115.3		
$(\mathbf{1X})_3$	–137.0	–155.1			–134.2	–153.1		
$(\mathbf{1X})_4$	–147.1	–167.3	–157.9		–144.7	–165.6	–151.9	
$(\mathbf{1X})_5$	–153.6	–173.1	–170.0	–218.4	–151.4	–171.7	–165.6	–220.4

$(\mathbf{1X})_6$	–158.0	–175.7	–174.6	–197.9	–156.0	–174.5	–172.4	–206.4
$(\mathbf{1X})_7$	–161.2	–177.4	**–176.4**	–186.7	–159.4	–176.0	–175.1	–191.0
$(\mathbf{1X})_8$	–163.7	–178.1	–176.1	–174.2	–161.9	–176.8	**–175.6**	–179.1
$(\mathbf{1X})_9$	–165.6	–179.0	–175.2	–167.8	–163.9	–178.2	–175.3	–173.0
$(\mathbf{1X})_{10}$	–167.1	–179.0	–175.6	–173.9	–162.5	–178.0	–174.6	–168.4

From the values in Table 2 it is clear that the largest cooperative effect is observed on going from the dimers to the trimers. Also, both the energy per monomer and the incremental interaction energy (Table 2 and Figure 6) in the linear clusters show that cooperative effects are practically saturated in the decamer. A graphical representation of the evolution of the average interaction energy per monomers with the cluster size is shown in Figure 6.

In contrast, the interaction energy per monomer in the cyclic structures presents a maximum in the heptamer for the parent and in the octamer for the fluorinated derivative. Interestingly, however, in contrast with the linear complexes, for the cyclic clusters the variation of the interaction energy with the size of the cluster steadily decreases.

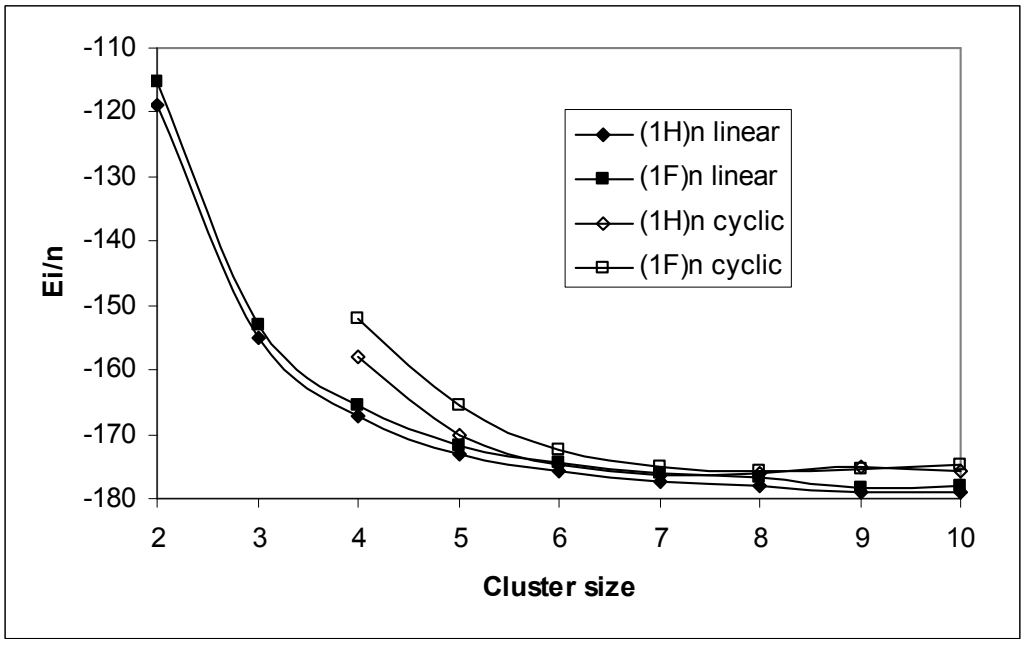

Figure 6. Evolution of the average interaction energy per monomer (Eq. 2) in the linear and cyclic clusters.

AIM analysis

The topological analysis of the electron density of the systems shows the presence of intermolecular bond critical points (BCP) and the corresponding bond path between the Be and N atoms, in agreement with the NBO description discussed in previous sections. The values of the electron density at the BCP, ρ_{BCP}, which range between 0.082 and 0.063 au, and those of the Laplacian at the BCP, ranging between 0.477 and 0.370 au, are characteristic of closed-shell interactions as those expected between two groups which behave as a Lewis base and a Lewis acid, respectively. The representation of the values of the ρ_{BCP} vs. the corresponding interatomic distances shows a clear dependence of the values with the substituent attached to the beryllium atom (H or F) (Figure 7). Thus, two independent correlations are obtained. A similar feature is observed for the C-Be bonds, but in this case the differences between the ρ_{BCP} due to the substitution in the beryllium atom are not as important as in the B···N bonds.

The exponential relationships found between the ρ_{BCP} and the interatomic distances are similar to those described for other weak interactions.[80-84]

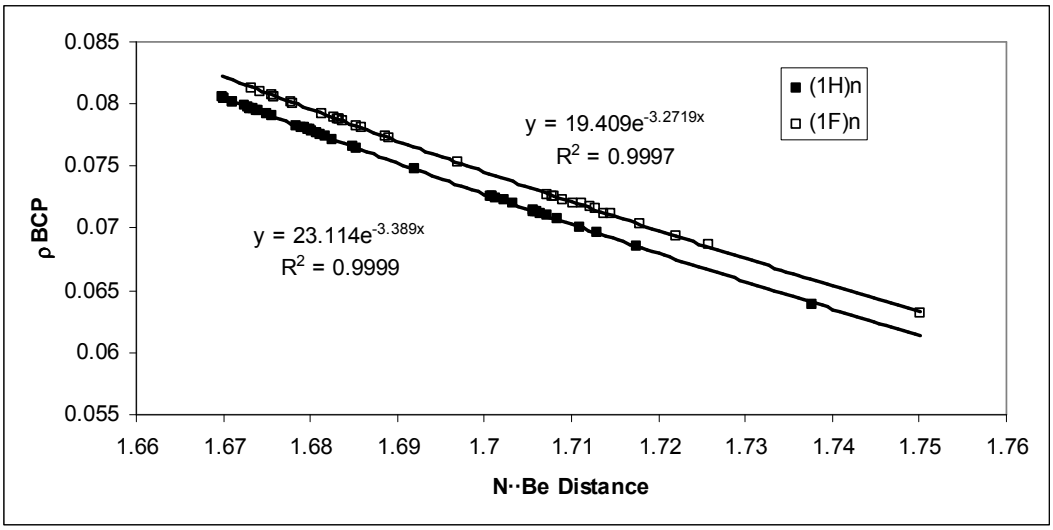

Figure 7. ρ_{BCP} (au) vs. N···Be interatomic distance (Å) in the clusters here studied.

NMR properties: absolute chemical shieldings.

The ^{13}C, ^{15}N and ^{9}Be absolute chemical shieldings of the different complexes have been calculated. The ^{13}C shieldings range between –10.5 to –50.8 ppm in the **1H** series and between –0.7 and –41.9 ppm in the **1F** one. Like in the case of the bond distances, the

chemical shielding depends on the size of the cluster examined and the position of the atom (monomer) along the chain (Figure 8 and S4 of the SI). Thus, the shielding of the carbon atoms in the extreme of the chain is clearly different to that of the carbon atoms in the central monomers. In addition, a size effect is observed and the shielding of the carbon atoms in larger chains is more negative than similar ones in smaller chains. All these findings are in nice agreement with the charge redistribution discussed in previous sections

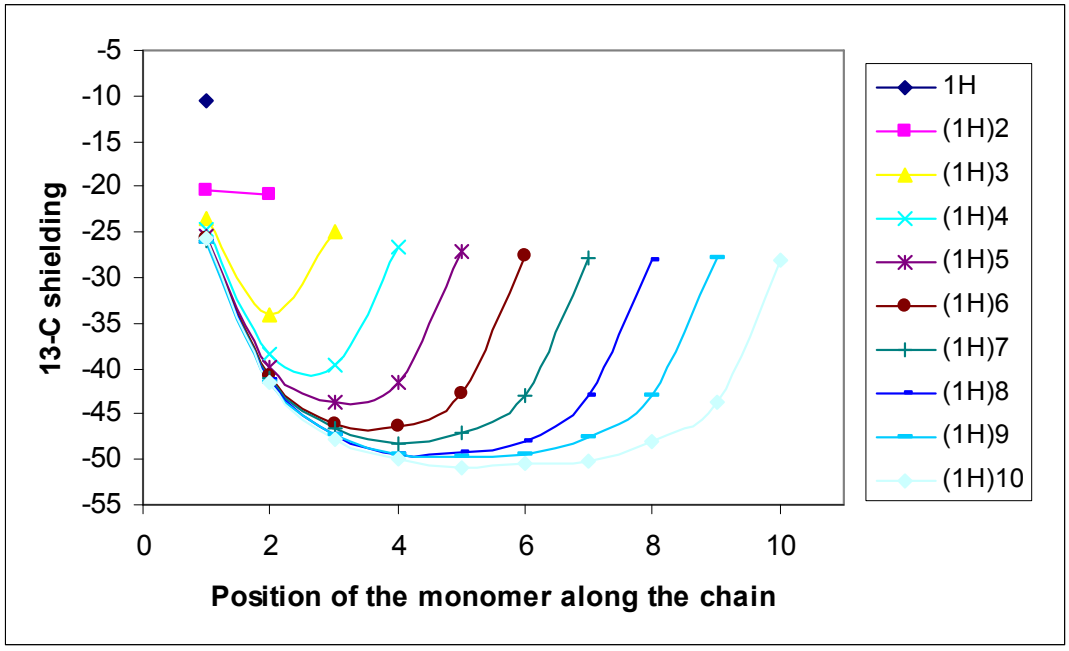

Figure 8. Absolute chemical shieldings of the C atoms vs. the position of the monomers in the chain for the **1H** series. The corresponding figure for the **1F** series is reported in the SI (Figure S3).

The complexation has an important influence in the ^{15}N chemical shielding. Thus, those nitrogen atoms not involved in the beryllium bond (terminal monomer) show shielding between –171.8 and –150.7 ppm in the **1H** series (between –183.4 and –146.4 ppm in the **1F** series) while those involved in the interaction between –57.5 and –30.2 ppm (between –60.1 and –15.4 ppm in the **1F** series). In this case, the larger size of the cluster and the central position of the monomer favor a less negative shielding of the nitrogen atoms.

Finally, the absolute chemical shielding range for the beryllium atoms are only 5 ppm (between 98.2 and 93.1 ppm in the **1H** series and between 111.3 and 106.3 ppm in the **1F** one). In the **1H** series, the smallest value corresponds to the beryllium atom that

is not involved in the interaction (terminal BeH monomer) while the largest one corresponds to the monomer locate in the opposite side of the chain (terminal NH monomer) (Figure 9). In the **1F** series the evolution of the chemical shielding is similar to that discussed for the ^{13}C atoms.

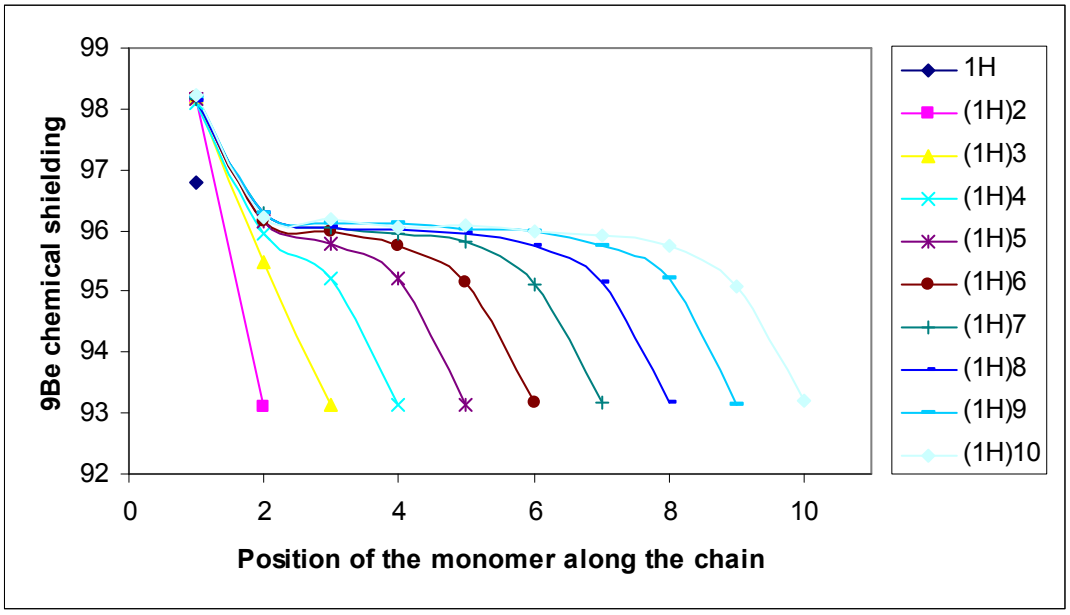

Figure 9. Evolution of the ^{9}Be chemical shielding in the **1H** series vs. the position along the chain.

Conclusions

A theoretical study of the cooperativity in beryllium bonds has been carried out by means of DFT computational methods. The structures of linear and cyclic cluster of two series of (iminomethyl)beryllium derivatives up to the decamer have been considered. The geometry, energy, electronic and NMR properties have been characterized and analyzed in order to obtain insight on the potential cooperativity in these clusters. All the results obtained indicate a positive cooperativity and its profile is similar to those described previously for hydrogen-bonded chains also with positive cooperativity. These results open also the possibility of generating new ditopic systems by introducing groups acting as Lewis bases as substituents in beryllium compounds, which behave as very strong Lewis acids, favoring the formation of new polymeric structures.

Acknowledgments

This work has been partially supported by the Ministerio de Economía y Competitividad (Project No. CTQ2012-35513-C02), the Project MADRISOLAR2, Ref.: S2009PPQ/1533 of the Comunidad Autónoma de Madrid, by Consolider on Molecular Nanoscience CSC2007-00010, and by the CMST COST Action CM1204. A generous allocation of computing time at the CTI (CSIC) and at the CCC of the UAM is also acknowledged. We warmly thank Prof. Frank A. Weinhold for his help with the NBO method.

References

1. M. Yáñez, P. Sanz, O. Mó, I. Alkorta and J. Elguero, *J. Chem. Theor. Comput.*, 2009, **5**, 2763-2771.
2. O. Mó, M. Yáñez, I. Alkorta and J. Elguero, *J. Chem. Theor. Comput.*, 2012, **8**, 2293-2300.
3. K. Eskandari, *J. Mol. Model.*, 2012, **18**, 3481-3487.
4. A. Martín-Sómer, A. M. Lamsabhi, O. Mó and M. Yáñez, *Comput. Theor. Chem.*, 2012, **998**, 74-79.
5. Q. Li, X. Liu, R. Li, J. Cheng and W. Li, *Spectrochim. Acta, Part A*, 2012, **90**, 135-140.
6. L. Albrecht, R. J. Boyd, O. Mó and M. Yáñez, *PCCP*, 2012, **14**, 14540-14547.
7. O. Mó, M. Yáñez, I. Alkorta and J. Elguero, *J. Mol. Model.*, 2013, **19**, 4139-4145.
8. M. Yáñez, O. Mó, I. Alkorta and J. Elguero, *Chem. Eur. J.*, 2013, **19**, 11637-11643.
9. M. M. Montero-Campillo, A. Lamsabhi, O. Mó and M. Yáñez, *J. Mol. Model.*, 2013, **19**, 2759-2766.
10. O. Mó, M. Yáñez, I. Alkorta and J. Elguero, *Mol. Phys.*, 2013, in press, DOI:10.1080/00268976.00262013.00843034.
11. M. Yáñez, O. Mó, I. Alkorta and J. Elguero, *Chem. Phys. Lett.*, 2013, **590**, 22-26.
12. L. R. MaCGillivray, *Metal-organic frameworks. Design and Application*, John Wiley & Sons, Singapore, 2010.
13. H. Kleeberg, D. Klein and W. A. P. Luck, *J. Phys. Chem.*, 1987, **91**, 3200-3203.
14. Y. Hannachi, B. Silvi and Y. Bouteiller, *J. Chem. Phys.*, 1992, **97**, 1911-1918.
15. O. Mó, M. Yáñez and J. Elguero, *J. Chem. Phys.*, 1992, **97**, 6628-6638.
16. A. Karpfen and O. Yanovitskii, *Theochem-J. Mol. Struct.*, 1994, **120**, 211-227.
17. S. Suhai, *Int. J. Quantum Chem.*, 1994, **52**, 395-412.
18. O. Mó, M. Yáñez and J. Elguero, *Theochem*, 1994, **120**, 73-81.
19. L. González, O. Mó, M. Yáñez and J. Elguero, *Theochem*, 1996, **371**, 1-10.
20. Z. Latajka and S. Scheiner, *Chem. Phys.*, 1997, **216**, 37-52.
21. G. S. Li, M. F. RuizLopez and B. Maigret, *J. Phys. Chem. A*, 1997, **101**, 7885-7892.
22. O. Mó, M. Yáñez and J. Elguero, *J. Chem. Phys.*, 1997, **107**, 3592-3601.
23. M. Lozynski, D. RusinskaRoszak and H. G. Mack, *J. Phys. Chem. A*, 1997, **101**, 1542-1548.
24. R. A. Bryce, M. A. Vincent, N. O. J. Malcolm, I. H. Hillier and N. A. Burton, *J. Chem. Phys.*, 1998, **109**, 3077-3085.

25. M. Masella and J. P. Flament, *J. Chem. Phys.*, 1998, **108**, 7141-7151.
26. L. González, O. Mó and M. Yáñez, *J. Chem. Phys.*, 1999, **111**, 3855-3861.
27. C. F. Guerra, F. M. Bickelhaupt, J. G. Snijders and E. J. Baerends, *Chem.-Eur. J.*, 1999, **5**, 3581-3594.
28. R. D. Parra and X. C. Zeng, *J. Chem. Phys.*, 1999, **110**, 6329-6338.
29. E. M. Cabaleiro-Lago and M. A. Rios, *J. Chem. Phys.*, 2000, **112**, 2155-2163.
30. R. D. Parra, B. Gong and X. C. Zeng, *J. Chem. Phys.*, 2001, **115**, 6036-6041.
31. L. Rincon, R. Almeida, D. Garcia-Aldea and H. D. Y. Riega, *J. Chem. Phys.*, 2001, **114**, 5552-5561.
32. S. Tsuzuki, H. Houjou, Y. Nagawa, M. Goto and K. Hiratani, *J. Am. Chem. Soc.*, 2001, **123**, 4255-4258.
33. J. J. Dannenberg, *J. Mol. Struct.*, 2002, **615**, 219-226.
34. A. Karpfen, in *Advances in Chemical Physics, Vol 123*, eds. I. Prigogine and S. A. Rice, John Wiley & Sons Inc, New York, 2002, vol. 123, pp. 469-510.
35. P. Raveendran and S. L. Wallen, *J. Am. Chem. Soc.*, 2002, **124**, 12590-12599.
36. H. Park and K. M. Merz, *J. Am. Chem. Soc.*, 2003, **125**, 901-911.
37. R. Wieczorek and J. J. Dannenberg, *J. Am. Chem. Soc.*, 2003, **125**, 14065-14071.
38. R. Viswanathan, A. Asensio and J. J. Dannenberg, *J. Phys. Chem. A*, 2004, **108**, 9205-9212.
39. E. D. Glendening, *J. Phys. Chem. A*, 2005, **109**, 11936-11940.
40. O. Mó, M. Yáñez, J. E. Del Bene, L. Alkorta and J. Elguero, *ChemPhysChem*, 2005, **6**, 1411-1418.
41. J. Kriz and J. Dybal, *J. Phys. Chem. B*, 2005, **109**, 13436-13444.
42. Y. F. Chen, R. Viswanathan and J. J. Dannenberg, *J. Phys. Chem. B*, 2007, **111**, 8329-8334.
43. V. S. Znamenskiy and M. E. Green, *J. Chem. Theory Comput.*, 2007, **3**, 103-114.
44. Q. Z. Li, X. L. An, F. Luan, W. Z. Li, B. A. Gong, J. B. Cheng and J. Z. Sun, *J. Chem. Phys.*, 2008, **128**, 6.
45. S. J. Grabowski and J. Leszczynski, *Chem. Phys.*, 2009, **355**, 169-176.
46. M. Nagaraju and G. N. Sastry, *Int. J. Quantum Chem.*, 2010, **110**, 1994-2003.
47. I. Alkorta, F. Blanco, P. M. Deyà, J. Elguero, C. Estarellas, A. Frontera and D. Quiñonero, *Theor. Chem. Acc.*, 2010, **126**, 1-14.
48. C. T. Lee, W. T. Yang and R. G. Parr, *Phys Rev B*, 1988, **37**, 785-789.
49. A. D. Becke, *J. Chem. Phys.*, 1993, **98**, 5648-5652.
50. P. C. Hariharan and J. A. Pople, *Theor Chim Acta*, 1973, **28**, 213-222.
51. M. J. Frisch, J. A. Pople and J. S. Binkley, *J. Chem. Phys.*, 1984, **80**, 3265-3269.
52. I. Rozas, I. Alkorta and J. Elguero, *J. Phys. Chem. A*, 1998, **102**, 9925-9932.
53. I. Alkorta, I. Rozas and J. Elguero, *Theor. Chem. Acc.*, 1998, **99**, 116-123.
54. M. J. Frisch, G. W. Trucks, H. B. Schlegel, G. E. Scuseria, M. A. Robb, J. R. Cheeseman, G. Scalmani, V. Barone, B. Mennucci, G. A. Petersson, H. Nakatsuji, M. Caricato, X. Li, H. P. Hratchian, A. F. Izmaylov, J. Bloino, G. Zheng, J. L. Sonnenberg, M. Hada, M. Ehara, K. Toyota, R. Fukuda, J. Hasegawa, M. Ishida, T. Nakajima, Y. Honda, O. Kitao, H. Nakai, T. Vreven, J. Montgomery, J. A., J. E. Peralta, F. Ogliaro, M. Bearpark, J. J. Heyd, E. Brothers, K. N. Kudin, V. N. Staroverov, R. Kobayashi, J. Normand, K. Raghavachari, A. Rendell, J. C. Burant, S. S. Iyengar, J. Tomasi, M. Cossi, N. Rega, N. J. Millam, M. Klene, J. E. Knox, J. B. Cross, V. Bakken, C. Adamo, J. Jaramillo, R. Gomperts, R. E. Stratmann, O. Yazyev, A. J. Austin, R. Cammi, C.

Pomelli, J. W. Ochterski, R. L. Martin, K. Morokuma, V. G. Zakrzewski, G. A. Voth, P. Salvador, J. J. Dannenberg, S. Dapprich, A. D. Daniels, Ö. Farkas, J. B. Foresman, J. V. Ortiz, J. Cioslowski and D. J. Fox, Gaussian, Inc., Wallingford CT, 2009.
55. R. F. W. Bader, *Atoms in Molecules. A Quantum Theory*, Clarendon Press, Oxford, 1990.
56. C. F. Matta and R. J. Boyd, *The Quantum Theory of Atoms in Molecules*, Wiley-VCH, Weinheim, 2007.
57. A. E. Reed, L. A. Curtiss and F. Weinhold, *Chem. Rev.*, 1988, **88**, 899-926.
58. J. R. Cheeseman, M. T. Carroll and R. F. W. Bader, *Chem. Phys. Lett.*, 1988, **143**, 450-458.
59. M. T. Carroll, C. Chang and R. F. W. Bader, *Mol. Phys.*, 1988, **63**, 387-405.
60. M. T. Carroll and R. F. W. Bader, *Mol. Phys.*, 1988, **65**, 695-722.
61. P. L. A. Popelier and R. F. W. Bader, *Chem. Phys. Lett.*, 1992, **189**, 542-548.
62. U. Koch and P. L. A. Popelier, *J. Phys. Chem.*, 1995, **99**, 9747-9754.
63. S. J. Grabowski and M. Malecka, *J. Phys. Chem. A*, 2006, **110**, 11847-11854.
64. A. Bil and Z. Latajka, *J. Comput. Chem.*, 2006, **27**, 287-295.
65. C. X. Xue and P. L. A. Popelier, *J. Phys. Chem. B*, 2008, **112**, 5257-5264.
66. F. Fuster and S. J. Grabowski, *J. Phys. Chem. A*, **115**, 10078-10086.
67. S. J. Grabowski, *J. Phys. Chem. A*, **115**, 12789-12799.
68. G. Sanchez-Sanz, C. Trujillo, I. Alkorta and J. Elguero, *ChemPhysChem*, **13**, 496-503.
69. T. A. Keith, TK Gristmill Software, Overland Park KS, USA, 11.10.16 edn., 2011 Version p. (aim.tkgristmill.com).
70. K. B. Wiberg, *Tetrahedron*, 1968, **24**, 1083-1088.
71. E. D. Glendening, J. K. Badenhoop, A. E. Reed, J. E. Carpenter, J. A. Bohmann, C. M. Morales, C. R. Landis and F. Weinhold, *NBO 6.0; University of Wisconsin: Madison, WI, 2013.*
72. Jmol:, *an open-source Java viewer for chemical structures in 3D, version 13.0. http://www.jmol.org/ (accessed on September 26th, 2013).*
73. M. Patek, *"Jmol NBO Visualization Helper" program. http://www.marcelpatek.com/nbo/nbo.html (accessed on September 26th, 2013).*
74. F. London, *Journal de Physique et le Radium*, 1937, **8**, 397-409.
75. R. Ditchfie, *Mol. Phys.*, 1974, **27**, 789-807.
76. Y.-F. Chen and J. J. Dannenberg, *J. Am. Chem. Soc.*, 2006, **128**, 8100-8101.
77. M. Sánchez, P. F. Provasi, G. A. Aucar, I. Alkorta and J. Elguero, *J. Phys. Chem. B*, 2005, **109**, 18189-18194.
78. I. Alkorta, J. Elguero and M. Solimannejad, *J. Chem. Phys.*, 2008, **129**, 064115.
79. I. Alkorta, F. Blanco and J. Elguero, *J. Phys. Chem. A*, 2010, **114**, 8457-8462.
80. J. E. Del Bene, I. Alkorta, G. Sanchez-Sanz and J. Elguero, *J. Phys. Chem. A*, 2011, **115**, 13724-13731.
81. G. Sánchez-Sanz, C. Trujillo, I. Alkorta and J. Elguero, *ChemPhysChem*, 2012, **13**, 496-503.
82. I. Mata, I. Alkorta, E. Molins and E. Espinosa, *Chem. Eur. J.*, 2010, **16**, 2442-2452.
83. O. Picazo, I. Alkorta and J. Elguero, *J. Org. Chem.*, 2003, **68**, 7485-7489.
84. I. Rozas, I. Alkorta and J. Elguero, *Chem. Phys. Lett.*, 1997, **275**, 423-428.